

# Single-Phase Photovoltaic Energy Conversion System Based on a New Maximum-Power-Point-Tracking Algorithm

Domenico Casadei, Gabriele Grandi, Claudio Rossi  
DEPT. OF ELECTRICAL ENGINEERING  
University of Bologna  
viale Risorgimento, 2 - 40136, Bologna ITALY  
*elettro@mail.ing.unibo.it*

Keywords: Active filters, Power conditioning, Renewable energy systems, Single phase systems, Solar Cell Systems

## Abstract

A new maximum power point tracking algorithm for single-stage converters connecting photovoltaic panels to a single-phase grid is presented. The algorithm is based on the analysis of the current and voltage low-frequency oscillations introduced in the PV panels by the single-phase utility grid. The proposed control technique allows the generation of sinusoidal grid currents with unity power factor. The proposed algorithm has been developed to allow an array of PV modules to be connected to the grid by using a single-stage converter. This simple structure yields higher efficiency and reliability when compared with standard solutions based on a two-stage converters configuration. The proposed maximum power point tracking algorithm has been numerically simulated and experimentally implemented by means of a converter prototype connected to a single-phase grid. Numerical and experimental results are presented in the paper, showing the effectiveness of the proposed system.

## I. Introduction

Photovoltaic technology is the most promising candidate for the large scale spreading of renewable energy source. Photovoltaic roofs give an important share of new installations of PV panels. For these applications the rated power is lower than 5 kW and the PV panels are permanently connected to a single-phase grid. The power flow between the PV panels and the grid is controlled by a power conditioning system (PCS), which should be reliable and inexpensive. To obtain the maximum efficiency of the system, the PCS must keep the power extracted from the PV panels close to the maximum power point (MPP). Several solutions for PCS with maximum power point tracking (MPPT) capability have been recently proposed, based on both single-stage [1] and double-stage converter topologies [2].

This paper deals with a single-phase, single-stage PCS configuration, employing a simple and effective MPPT embedded algorithm. The scheme of the proposed system is shown in Fig. 1. The output of the PV panels is directly connected to the dc-link of the inverter (VSI type), whereas the output of the inverter is connected to the grid through the ac-link inductor  $L_{ac}$ .

The VSI output voltage  $v_F$  is controlled in order to force the current injected into the mains  $i_S$  to follow a sinusoidal reference waveform, synchronized and in phase with the fundamental component of the source voltage  $v_S$ . As a consequence, a sinusoidal current is obtained even in presence of voltage perturbations coming from the mains [3].

The amplitude of the reference source current  $I_S^*$  is generated by the dc-link voltage regulator on the basis of the error between the dc-link voltage  $V_{dc}$  and the reference dc voltage  $V_{dc}^*$  of the PV panels.

The MPPT algorithm varies  $V_{dc}^*$  according to the environmental conditions in order to keep the operating point of the PV panels close to the maximum power point.

The basic principle of the MPPT algorithm is to

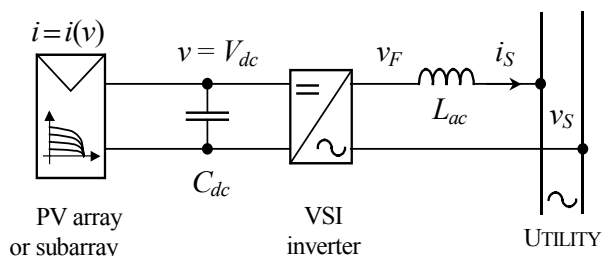


Fig. 1 - Schematic diagram of the PV generation system

exploit current and voltage oscillations caused by the instantaneous power pulsations related to the active power injected into the single-phase grid. Analyzing these oscillations it is possible to obtain information about the power gradient, evaluating if the PV system operates close to the maximum power point.

As it is known, for a non-null value of active power injected into the mains  $P_S$ , the instantaneous power  $p_S(t)$  pulsates at a frequency twice than that of the grid. If the current  $i_S(t)$  is in phase agreement with the source voltage  $v_S(t)$ , the instantaneous value of power injected into the mains is

$$p_S(t) = v_S(t)i_S(t) = \sqrt{2}V_S \cos \omega t \sqrt{2}I_S \cos \omega t = V_S I_S (1 + \cos 2\omega t). \quad (1)$$

The average quantity  $V_S I_S$  corresponds to the active power  $P_S$ . The power pulsation at frequency  $2\omega$  in (1) is reflected on the dc-link bus of the VSI as a voltage pulsation superimposed to the average of the dc-link voltage  $V_{dc}$ . The variation of  $V_{dc}$  can be related to active power  $P_S$ , grid frequency  $\omega$ , and dc-link capacitor  $C_{dc}$  by the following relationship:

$$\frac{P_S}{\omega} = C_{dc} (V_{dcMAX}^2 - V_{dcMIN}^2). \quad (2)$$

The dc-link voltage excursion  $V_{dcMAX} - V_{dcMIN}$  can be limited by choosing a proper value for  $C_{dc}$ , according with (2), ensuring the correct operation of the inverter. The residual oscillation of  $V_{dc}$  determines a small pulsation of power supplied by the PV panels. On the basis of the phase relationship between power and voltage oscillations, the MPPT algorithm moves the operating point of the PV panels by varying  $V_{dc}^*$  until the MPP is reached. Voltage and current oscillations must be as small as possible in order to minimize the oscillation of power extracted from the panel. On the other hand, these oscillations must be large enough to be sensed and distinguished from current and voltage ripple due to the VSI switching effects. It has been observed that keeping voltage and current oscillation around 1% of their rated values leads to a good behavior of the whole PV generation system.

The capability of the proposed system to keep under control the power injected into the grid for any operating condition is ensured by the use of a reliable synchronizing device and an effective current regulator applied to the current injected into the grid. In particular, the synchronization of the inverter output voltages with the fundamental component of the source voltages is carried out by a phase locked loop (PLL). Then, the proposed algorithm operates correctly even in presence of non-sinusoidal source voltages. The current regulator could be realized in different ways. In this paper a predictive PWM current regulator has been utilized.

## II. Proposed MPPT algorithm

The aim of any MPPT algorithm is to extract the maximum power from the PV panels. Usually, the condition  $\partial p / \partial v = 0$  is adopted to locate this operating point, since PV panels show a unique global maximum power point.

The proposed MPPT algorithm is based on the determination of the slope of the PV panels output power versus voltage, i.e., the power derivative  $\partial p / \partial v$ . This quantity is utilized as representative of the “voltage error”, i.e., the difference between the actual voltage of the PV panels and the reference voltage  $v^*$  corresponding to the maximum power operating point. The qualitative behavior of  $\partial p / \partial v$  is represented in Fig. 2: in the region nearby  $v^*$  the power derivative can be considered a straight line having the slope  $k$ .

In order to determine the power derivative  $\partial p / \partial v$  it is necessary to introduce a voltage and current perturbation around any operating point of the PV array. Traditional MPPT algorithms are based on “perturbation and observation” method or “incremental conductance” method. Some variants to these methods have been presented in order to improve the dynamic performance and/or to reduce undesired oscillations around the MPP [1], [4], [5]. Alternative methods are based on measuring and processing the current and/or voltage ripple due to the switching behavior of the converter connected to the PV panels array [6]-[8]. For small PV power applications, high switching frequency converters are usually adopted, reducing the residual voltage and current ripple below practical exploitable values. In this paper the oscillation of the instantaneous power due to the connection of the PV system to a single-phase

grid can be considered itself as an embedded dynamic test signal useful to determine  $\partial p/\partial v$ . A key feature of this method is the knowledge of the oscillations period  $T = 1/(2f)$  to improve the MPPT algorithm performances, being  $f$  the grid frequency.

In order to derive the proposed MPPT algorithm, let us consider a periodic function  $x(t)$  having the moving average component  $\bar{x}(t)$  over the period  $T$ , and the alternative component  $\tilde{x}(t)$ , respectively defined as

$$\bar{x}(t) = \frac{1}{T} \int_{t-T}^t x(\tau) d\tau, \quad (3)$$

$$\tilde{x}(t) = x(t) - \bar{x}(t). \quad (4)$$

Applying these definitions to the output voltage and power of the PV panels, leads to

$$v(t) = \bar{v}(t) + \tilde{v}(t), \quad (5)$$

$$p(t) = \bar{p}(t) + \tilde{p}(t). \quad (6)$$

The average operating point  $(v_o, p_o)$  on the  $p = p(v)$  characteristic, and the corresponding voltage and power alternative components are represented in Fig. 2, according to the following expressions:

$$\bar{p}(t) = p(\bar{v}(t)) = p(v_o), \text{ being } v_o = \bar{v}(t). \quad (7)$$

Assuming the curve  $p = p(v)$  still valid for dynamic analysis [7] and linearizing nearby the average operating point  $p_o = p(v_o)$  leads to a simple relationship between the power ripple and the voltage ripple, expressed as

$$\tilde{p}(t) \cong \left( \frac{\partial p}{\partial v} \right)_{v_o} \tilde{v}(t). \quad (8)$$

The power derivative can be calculated by (8) as a function of power and voltage oscillations around the given operating point  $(v_o, p_o)$ . In order to avoid critical calculations based on instantaneous power and voltage values [9], it is possible to introduce instead of (8) the moving average of the product of (8) and  $\tilde{v}(t)$ , leading to

$$\int_{t-T}^t \tilde{p}(\tau) \tilde{v}(\tau) d\tau \cong \left( \frac{\partial p}{\partial v} \right)_{v_o} \cdot \int_{t-T}^t \tilde{v}^2(\tau) d\tau. \quad (9)$$

Then, the power derivative can be evaluated as the following ratio:

$$\left( \frac{\partial p}{\partial v} \right)_{v_o} \cong \frac{\int_{t-T}^t \tilde{p}(\tau) \tilde{v}(\tau) d\tau}{\int_{t-T}^t \tilde{v}^2(\tau) d\tau}. \quad (10)$$

It can be noted that in (10) the power derivative is expressed in terms of integral quantities.

The voltage and power alternative components utilized in (10) can be evaluated on the basis of (3) and (4), leading to

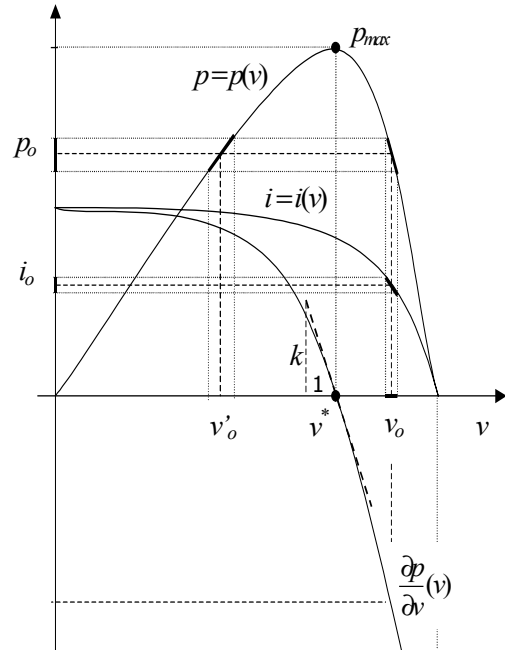


Fig. 2 - Current, power, and power derivative of the PV panels vs. voltage

$$\tilde{v}(t) = v(t) - \frac{1}{T} \int_{t-T}^t v(\tau) d\tau \quad (11)$$

$$\tilde{p}(t) = p(t) - \frac{1}{T} \int_{t-T}^t p(\tau) d\tau. \quad (12)$$

In order to implement the proposed algorithm, a traditional filtering approach can be usefully adopted to extract the alternative components. In particular, high-pass filters (HPF) can be used instead of (11) and (12). In the same way, low-pass filters (LPF) can be used instead of the moving averaging integrals of (10). The corresponding block diagram is depicted in Fig. 3.

The power derivative  $\partial p/\partial v$  computed by the MPPT algorithm represents the voltage error  $\Delta v = v^* - v$ , i.e., the distance between the MPP voltage and the actual voltage, since the relationship between power and voltage is almost linear in the region around the MPP, as shown in Fig.2.

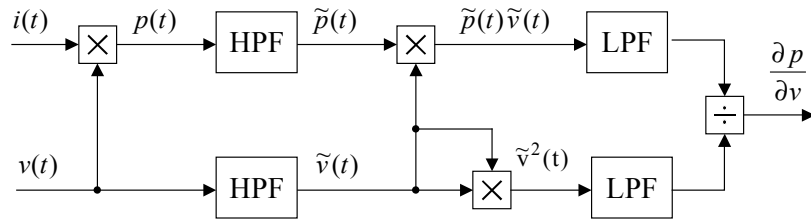


Fig. 3 - Estimation of the PV power derivative by using filtering blocks.

### III. Implementation

The block diagram shown in Fig. 3 can be simplified in order to be easily implemented on a low cost DSP, without reducing the performances of the MPPT algorithm. In particular, the average of the product  $\tilde{p} \cdot \tilde{v}$  could be conveniently utilized as the input variable of the dc-link voltage regulator. In fact, on the basis of (10), being the integral at the right-hand side always greater than zero, the sign of the integral at the left-hand side corresponds to the sign of the power derivative  $\partial p/\partial v$ :

$$\text{sign} \left( \int_{t-T}^t \tilde{p}(t)\tilde{v}(t) dt \right) = \text{sign} \left( \frac{\partial p}{\partial v} \right). \quad (13)$$

The quantity  $\text{sign}(\partial p/\partial v)$  is a clear indication of the region where the PV panel is working.

- $(\partial p/\partial v) > 0$  means  $\tilde{p}$  and  $\tilde{v}$  in phase agreement. The operating point is on the left side of the MPP on the  $I$ - $V$  characteristic;
- $(\partial p/\partial v) < 0$  means  $\tilde{p}$  and  $\tilde{v}$  in phase opposition. The operating point is on the right side of the MPP on the  $I$ - $V$  characteristic.

The instantaneous knowledge of the operating point region makes it possible to change the dc-link voltage reference in order to approach the maximum power operating point. On the basis of these considerations, the scheme of Fig. 3 can be simplified as represented in Fig. 4, where only the quantity corresponding to the average of the product  $\tilde{p} \cdot \tilde{v}$  and its sign is computed. In particular, the sign is extracted by a hysteretic comparator, set by a small band around zero and with the output values  $[-1, 1]$  representing  $\text{sign}(\partial p/\partial v)$ .

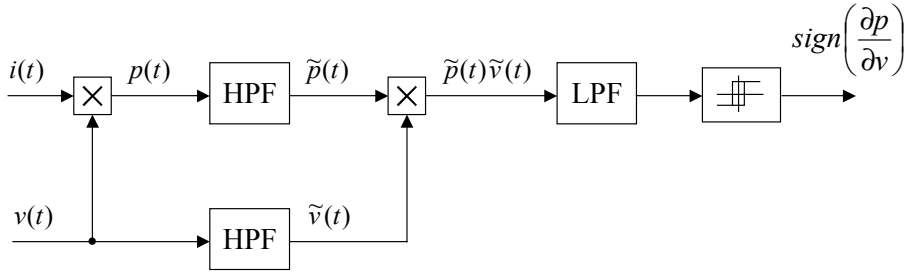


Fig. 4 - Simplified estimation of the PV power derivative by using filtering blocks

The scheme of the proposed dc-link voltage controller is represented in Fig. 5. When  $sign(\partial p/\partial v) > 0$  the integrator increases its output,  $\Delta V_{dc}$ , and the dc-link voltage reference  $V_{dc}^*$  moves towards the MPP. On the contrary, when  $sign(\partial p/\partial v) < 0$  the integrator decreases  $\Delta V_{dc}$  and the dc-link voltage reference  $V_{dc}^*$  moves back towards the MPP. The rate of change of  $V_{dc}^*$  is set by the gain  $K$ .

The input signal  $V_{dc}^{**}$  represents the initial voltage reference, i.e., the starting value of the integrator. When the control system is enabled, the quantity  $\Delta V_{dc}$  computed by the MPPT algorithm is added to  $V_{dc}^{**}$ , giving the actual reference of the dc-link voltage  $V_{dc}^*$ . Then, the regulation of the current  $i_S$  injected into the mains allows the dc-link voltage to be controlled around the reference value. In this way, all the power coming from the PV generator is transferred to the electric network. Following the reference value  $V_{dc}^*$  allows the PV panels to reach the maximum power operating point, where the condition  $\partial p/\partial v = 0$  is satisfied.

The desired amplitude of the source current,  $I_S^*$ , is generated by the regulator  $R(s)$ , considering the dc-link voltage error  $V_{dc} - V_{dc}^*$  as input variable. The reference value of the instantaneous source current  $i_S^*$  is generated on the basis of the amplitude  $I_S^*$ , and the phase angle of the fundamental component of the supply voltage  $v_S$ , which is represented by the unity sinusoid  $\hat{v}_S^1$  in Fig. 5 [10], [11].

The measurement of the source current is used to implement the ac current control loop. The inverter is controlled on the basis of the instantaneous current error  $\Delta i_S = i_S^* - i_S$  through a predictive PWM current regulator. In particular, the inverter reference voltage  $v_F^*$  can be calculated by the voltage equation written across the ac-link inductance  $L_{ac}$ , according with the block diagram represented in Fig. 1. Neglecting the resistive effects and introducing a variational model, this equation yields

$$v_F^* = v_S - \frac{L}{\Delta t} \Delta i_S \quad (13)$$

The parameter  $L/\Delta t$  in (13) can be adjusted to obtain the desired regulator performance.

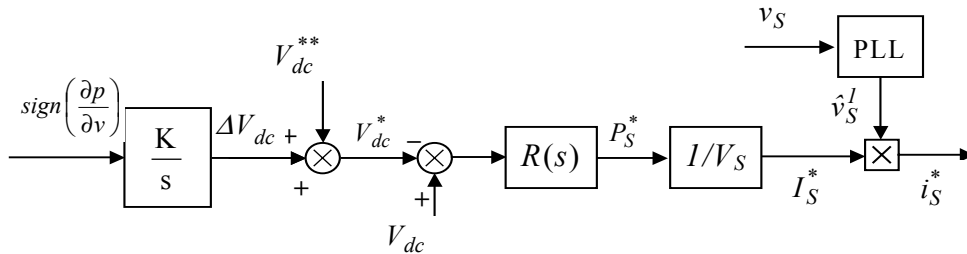


Fig. 5 - dc-link voltage reference generator and regulation scheme

## IV. System performance

### Simulation results

The proposed MPPT algorithm, summarized in Figs. 4 and 5, has been numerically simulated by using the Simulink environment of Matlab, with reference to a single-stage converter connected to a single-phase utility grid, as represented in Fig. 1. The PV panels have been electrically represented by the well-known single-exponential model [12], fitted on the  $I-V$  characteristic of a series array of ten modules Solar Shell SP150 type. The main characteristics of the PV generation system are summarized in Table I.

Rated power of the PV system	$P_{PV} = 1.5 \text{ kW}$	MPPT high pass filters: first order	$K_{HPF} = 1$ $\tau_{HPF} = 0.05 \text{ s}$
Dc-link capacitance	$C_{dc} = 2 \text{ mF}$	MPPT low pass filter: first order	$K_{LPF} = 1$ $\tau_{LPF} = 0.05 \text{ s}$
PWM carrier frequency	$f_{sw} = 10 \text{ kHz}$	Dc-link voltage controller: PI type	$K_p = 0.1$ $K_i = 10$
Ac-link inductor	$R_{ac} = 0.1 \text{ } \Omega$ $L_{ac} = 1 \text{ mH}$	Panels type (10 x, series connection)	Solar Shell SP150
Single phase utility grid (source)	$V_S = 230 \text{ V}$ $f = 50 \text{ Hz}$	Short circuit current (1000 W/m <sup>2</sup> , 40 °C)	$I_{sc} = 4.8 \text{ A}$
Dc-link initial reference voltage	$V_{dc}^{**} = 390 \text{ V}$	Open circuit voltage (1000 W/m <sup>2</sup> , 40 °C)	$V_{oc} = 420 \text{ V}$

The performance of the power conditioning system connected to the photovoltaic array has been evaluated both in steady state and transient operating conditions determined by start up and solar irradiance variations.

In Figs. 6-9 is represented the behaviour of the control system in steady state condition. In particular, Fig. 6 shows the behaviour of  $\tilde{v}$  and  $\tilde{p}$  around the maximum power point. Initially,  $\tilde{v}$  and  $\tilde{p}$  are in phase agreement, i.e., the operating point of the PV modules is on the left side of the MPP on the  $I-V$  characteristic. Successively,  $\tilde{v}$  and  $\tilde{p}$  become in phase opposition, i.e., the operating point of the PV modules is on the right side of the MPP on the  $I-V$  characteristic. For all the operating conditions the frequency of  $\tilde{v}$  and  $\tilde{p}$  is always twice than that of the grid frequency.

Fig. 7 shows the time behaviour of the dc-link voltage. The triangular oscillations are introduced by the hysteretic controller, whereas the sinusoidal oscillation are related to the instantaneous power exchange with the single-phase utility grid. The oscillation amplitude is lower than 1% of the voltage at the MPP. Fig. 8 shows the small effects of these oscillations in terms of PV instantaneous power.

In Fig. 9 the voltage and the grid current are represented in steady-state conditions. As expected, the current  $i_s$  injected into the grid is exactly in phase agreement with the grid voltage  $v_s$ .

Fig. 10 shows the performance of the PV generation system in tracking the maximum power point of the PV panels during a transient of solar irradiance. From the starting operating point ①, the system reaches the MPP in ②. Then, as a consequence of a 50% reduction of the solar irradiance, the operating points moves to the new MPP in ③.

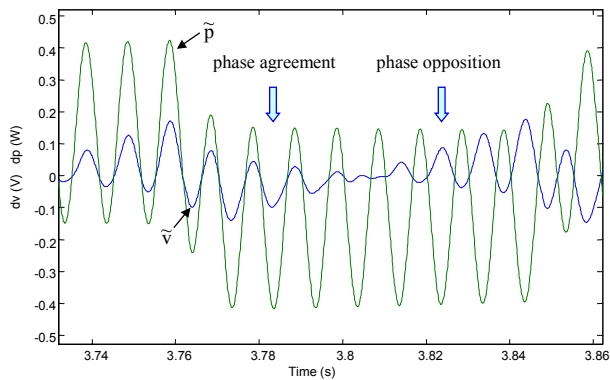


Fig. 6 - Alternative components of voltage and power,  $\tilde{v}$  and  $\tilde{p}$ .

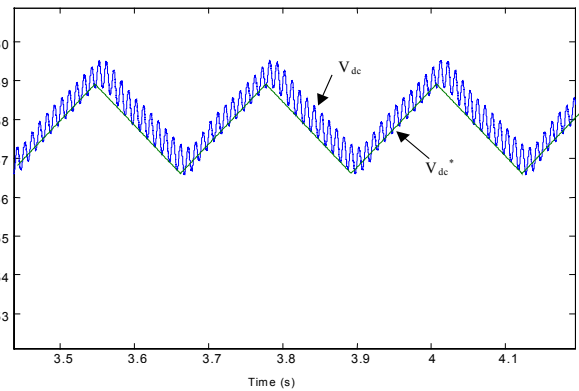


Fig. 7 - Dc-link voltage  $V_{dc}$  and dc-link voltage reference  $V_{dc}^*$ .

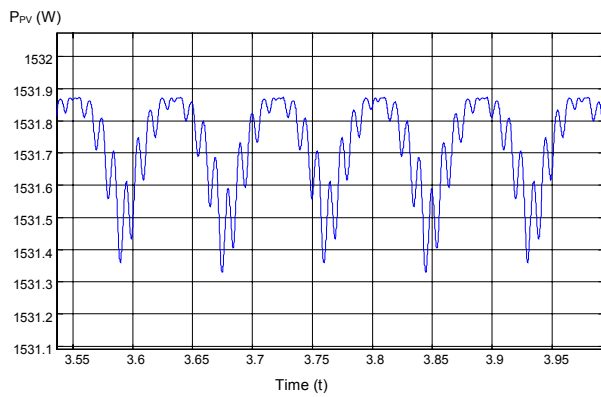


Fig. 8 - Instantaneous power supplied by the PV modules.

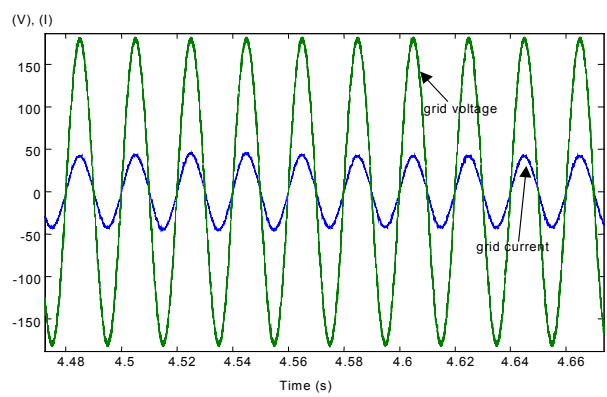


Fig. 9 - Grid voltage and grid current in steady-state conditions.

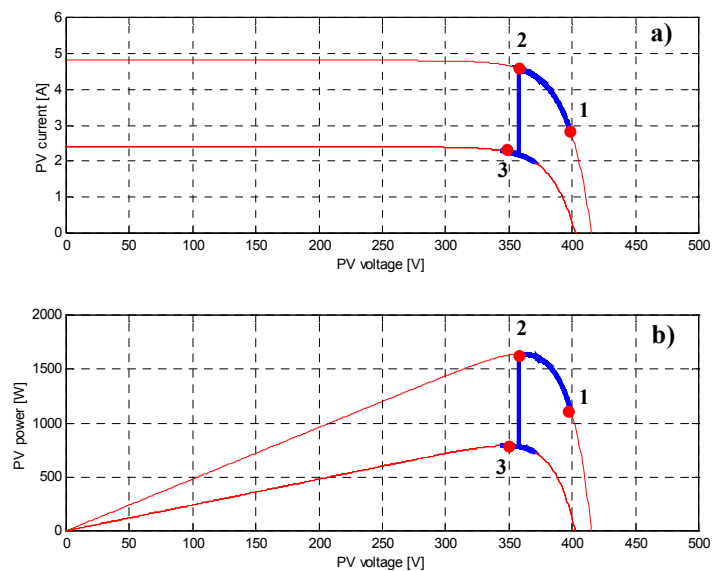


Fig. 10 - Effects of a 50% solar irradiance transient:  
 a) PV current vs. PV voltage  
 b) PV power vs. PV voltage

## V. Experimental results

The proposed control system for a single-phase, single-stage converter has been implemented on a laboratory prototype, where the PV panels have been replaced by an electric circuit, which behaves as a power generator having an  $I-V$  characteristic similar to that of the PV panels.

The  $P-V$  characteristic representing the PV panels is given in Fig. 11. In this case the MPP is achieved with a dc-link voltage of 250 V. Fig. 12 shows the steady-state waveforms of voltage and current at the utility grid side. It can be noted that the resulting source current  $i_s$  is sinusoidal and in phase agreement with the fundamental components of the source voltage  $v_s$ , although the source voltage has a low order harmonic distortion.

Figs. 13 and 14 show the behaviour of the proposed MMP algorithm during the start-up of the whole PV generation system. The output voltage of the power generator at the initial instant, when the converter is disabled, corresponds to the open circuit voltage (500 V). When the system is enabled the reference dc-link voltage moves from the starting value (400 V) towards the maximum power point (250 V). During the seeking of the MPP the dc-link voltage  $V_{dc}$  is always close to the reference voltage  $V_{dc}^*$  given by the MPPT algorithm. At the start-up, the dc-link voltage regulator guarantees the matching between the reference voltage  $V_{dc}^*$  and the dc-link voltage  $V_{dc}$  in about 0.2 s, then the MPP is reached in about 6 s.

Figs. 15 and 16 show the performance of the proposed MPPT algorithm in response to a step variation from 25 A to 20 A of the short circuit current of the generator, corresponding to a 20% decrease of the solar irradiance. The operating point moves from ① to the new MPP in ② in about 0.5 s. Once the new MPP is reached, only very small oscillations persist around the MPP.

## VI. Conclusion

A novel control strategy for single-stage converters connecting PV panels to a single-phase grid is proposed in this paper. The embedded MPPT algorithm is able to find the maximum power point by computing the sign of the PV power derivative. This computation exploits PV current and voltage oscillations, at a frequency twice than that of the grid, due to the connection of the converter with a single-phase grid. Then, the proposed MPPT algorithm does not require the knowledge of the model of the PV panels.

Once the maximum power point is computed by the MPPT algorithm, a dc-link voltage regulator drives the PV panels voltage to the MPP value. The current regulator ensures sinusoidal current and unity power factor for any operating condition.

The whole PV generation system has been numerically simulated and realized by a laboratory prototype showing the simple structure of the proposed control scheme.

Simulation and experimental results in steady-state and dynamic conditions have been also presented. The results show good performance of the control system and confirm the effectiveness of the proposed PV generation system for any operating condition.



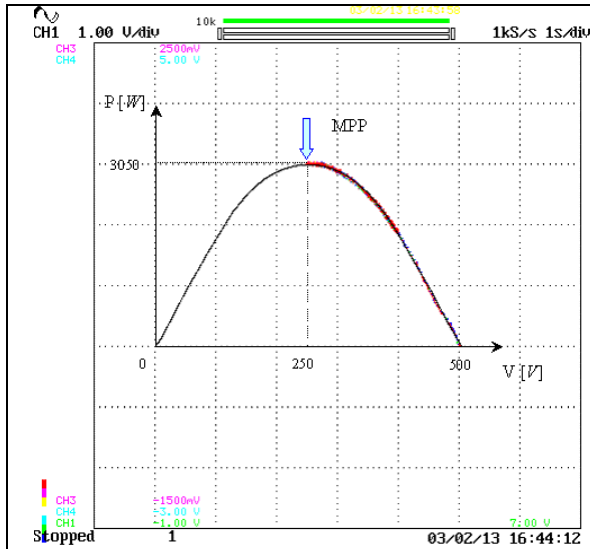


Fig. 11 -  $P$ - $V$  characteristic of the power generator replacing the PV panels.

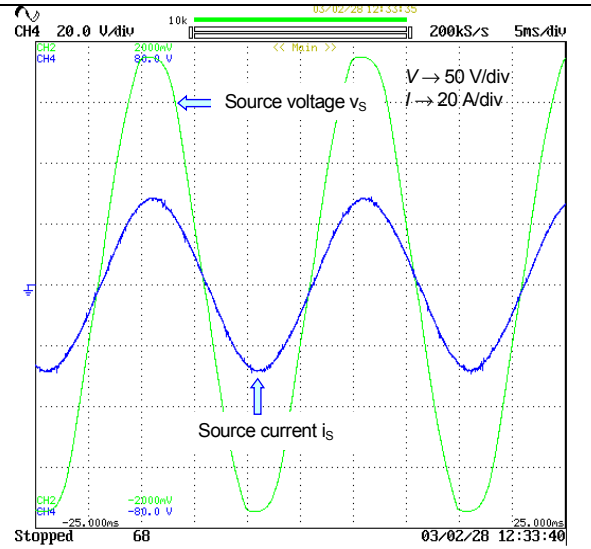


Fig. 12 - Source current  $i_s$  and source voltage  $v_s$  in steady-state condition.

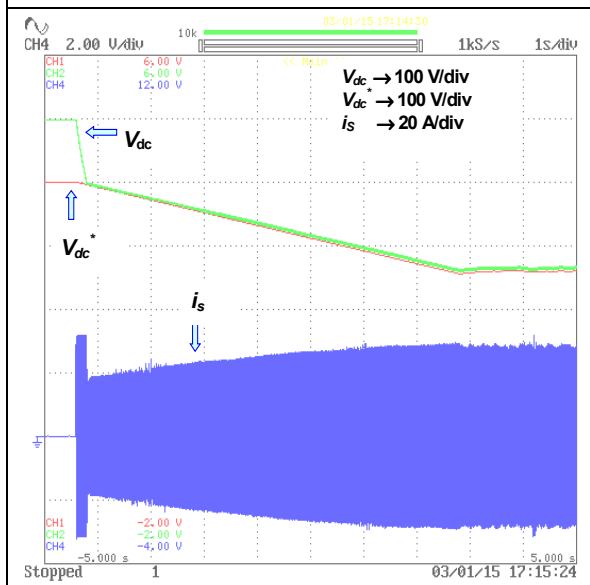


Fig. 13 -  $V_{dc}^*$ ,  $V_{dc}$ , and  $i_s$  during the start-up.

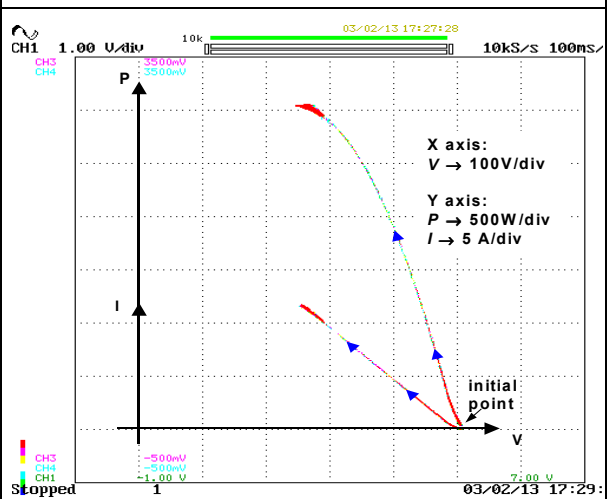


Fig. 14 -  $P$ - $V$  and  $I$ - $V$  characteristic representing the transient during the start-up of the PV generation system.

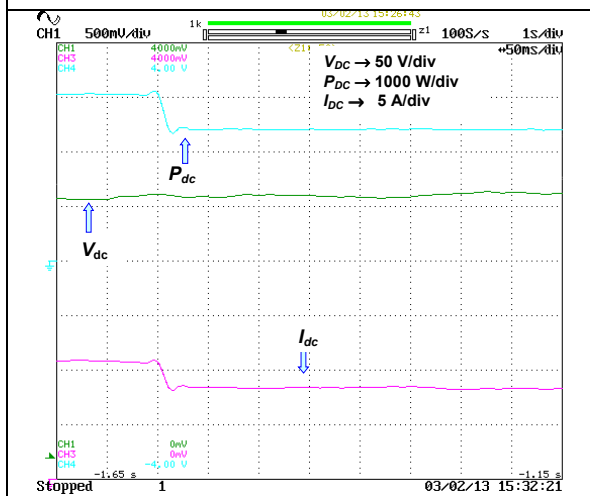


Fig. 15 - Voltage, current, and power supplied by the generator vs. time during a transient representing a step change of the solar irradiance.

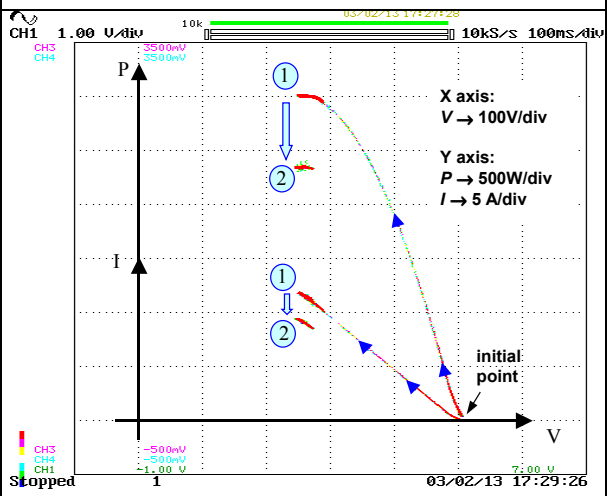


Fig. 16 -  $P$ - $V$  and  $I$ - $V$  characteristic during a step change of the solar irradiance.

## References

- [1] Y.C. Kuo, T.J. Liang, J.F. Chen, "Novel maximum-power-point-tracking controller for photovoltaic energy conversion system," *IEEE Trans. on Industrial Electronics*, Vol. 48 No. 3, June 2001, pp. 594-601
- [2] J.A. Gow, C.D. Manning, "Photovoltaic converter system suitable for use in small scale stand-alone or grid connected applications," *IEE Proceedings of Electric Power Applications*, Vol. 147, No. 6, Nov. 2000, pp. 535-543
- [3] D. Casadei, G. Grandi, C. Rossi, "Effects of Supply Voltage non-Idealities on the Behavior of an Active Power Conditioner for Cogeneration Systems", *Proc. of IEEE Power Electronic Specialist Conference, PESC*, Galway (Ireland), 18-23 June, 2000
- [4] T.Y. Kim, H.G. Ahn, S.K. Park, Y.K. Lee, "A novel maximum power point tracking control for photovoltaic power system under rapidly changing solar radiation," *Proc. of IEEE International Symposium on Industrial Electronics*, ISIE 2001, Pusan, Korea, Vol. 2, pp. 1011-1014
- [5] J.A. Gow, C.D. Manning, "Controller arrangement for boost converter systems sourced from solar photovoltaic arrays or other maximum power sources," *IEE Proceedings of Electric Power Applications*, Vol. 147, No. 1, Jan. 2000, pp. 15-20
- [6] A. Brambilla, M. Gambarara, A. Garutti, F. Ronchi, "New approach to photovoltaic arrays maximum power point tracking," *Proc. of 30<sup>th</sup> Annual IEEE Power Electronics Specialists Conference, PESC 1999*, Vol. 2, pp. 632-637
- [7] P. Midya, P.T. Krein, R.J. Turnbull, R. Reppa, J. Kimball, "Dynamic maximum power point tracker for photovoltaic applications," *Proc. of 27<sup>th</sup> Annual IEEE Power Electronics Specialists Conference, PESC 1996*, Vol. 2, pp. 1710-1716
- [8] D.L. Logue, P.T. Krein, "Optimization of power electronic systems using ripple correlation control: a dynamic programming approach," *Proc. of IEEE 32<sup>nd</sup> Annual Power Electronics Specialists Conference, PESC 2001*, Vol. 2, pp. 459-464
- [9] Y.H. Lim, D.C. Hamill, "Synthesis, simulation and experimental verification of a maximum power point tracker from nonlinear dynamics," *Proc. of IEEE 32<sup>nd</sup> Annual Power Electronics Specialists Conference, PESC 2001*, Vol. 1, pp. 199-204
- [10] D. Casadei, G. Grandi, C. Rossi, "Dynamic Performance of a Power Conditioner Applied to Photovoltaic Sources" *Proc. of EPE-PEMC'01, Cavtat (Croatia)*, Sept. 2002
- [11] G. Grandi, M. Landini, D. Casadei, C. Rossi: "Integration of photovoltaic sources and power active filters", *Proc. of 4th ISES Europe Solar Congress, EuroSun 2002, Bologna (Italy)*, June 23-26, 2002.
- [12] M.A. de Blas, J.L. Torres, E. Prieto, A. García: "Selecting a suitable model for characterizing photovoltaic devices," *Renewable Energy Journal*, Vol. 25, No. 3, March 2002, pp. 371-380.